CHAPTER-IV

Conductance, a Contrivance to Explore Ion Association and Solvation Behavior of an Ionic Liquid (Tetrabutylphosphonium Tetrafluoroborate) in Acetonitrile, Tetrahydrofuran, 1,3-Dioxolane and Their Binaries

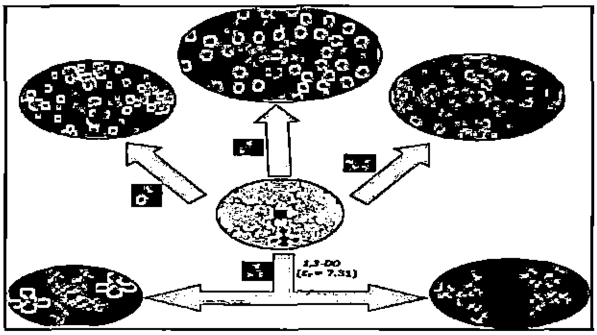

Precise measurements on electrical conductance (Λ) of solutions of an ionic liquid (IL) tetrabutylphosphonium tetrafluoroborate in acetonitrile (ACN), tetrahydrofuran (THF), 1,3-dioxolane (1,3-DO) and their binary mixtures have been reported at 298.15K. The conductance data have been analyzed by the Fuoss conductance equation (1978) in terms of the limiting molar conductance (Λ_o), the association constant (K_A), and the association diameter (R) for ion-pair formation. The Walden product is obtained and discussed. However, the deviation of the conductometric curves (Λ vs $\sqrt{c}$) from linearity for the electrolyte in THF and 1,3-DO and their binary mixtures indicated triple-ion formation and therefore corresponding conductance data have been analyzed by the Fuoss-Kraus theory of triple-ions. The limiting ionic conductances ($\lambda_o^{\pm}$) have been estimated from the appropriate division of the limiting molar conductivity value of tetrabutylammonium tetraphenylborate [Bu_4NBPh_4] as the "*reference electrolyte*" method along with a numerical evaluation of ion-pair and triple-ion formation constants ($K_P \approx K_A$ and K_T). The results have been discussed in terms of solvent properties and configurational theory. Ionic association in the limiting molar conductances, as well as the single-ion conductivity values have been determined for the electrolyte in the solvent media.

Ch-IV | Published in J. Physical Chemistry B, 2012, 116, 11687-11694.

IV.1. INTRODUCTION

In recent years, ionic liquids (ILs) have been considered attractive compounds due to their unique intrinsic properties, such as negligible vapour pressure, large liquid range, ability of dissolving a variety of chemicals, high thermal stability, large electrochemical window and their potential as 'designer solvents' and 'green' replacements for volatile organic solvents[IV.1-IV.3] used in reactions involving inorganic and bio-catalysis etc. They are also used as heat transfer fluids for processing biomass and as electrically conductive liquids in electrochemistry (batteries and solar cells).[IV.4- IV.6] In the modern technology, the application of the salt is well understood by studying the ionic solvation or ion association.

Consequently, a number of conductometric[IV.7] and related studies of electrolytes in non-aqueous solvents, especially mixed organic solvents, have been made for their optimal use in high-energy batteries[IV.8] and for further more understanding organic reaction mechanisms.[IV.9] Ionic association of electrolytes in solution depends upon the mode of solvation of its ions[IV.10- IV.13] which in turn depends on the nature of the solvent/solvent mixtures. Such solvent properties as viscosity and the relative permittivity have been taken into consideration as these properties help in determining the extent of ion association and the solvent-solvent interactions. The non-aqueous system has been of immense importance[IV.14, IV.15] to the technologist and theoretician as many chemical processes occur in these systems. Thus, extensive studies on electrical conductance in various mixed organic solvents have been performed in recent years[IV.16- IV.20] to examine the nature and magnitude of ion-ion and ion-solvent interactions.

In continuation of our investigations on electrical conductance,[IV.17, IV.18, IV.21] an attempt has been made in the present study, to ascertain the nature of ion–solvent interactions of ionic liquid (IL) Tetrabutylphosphonium Tetrafluoroborate [Bu_4PBF_4] in polar aprotic solvents pure acetonitrile, tetrahydrofuran, 1,3-dioxolane and their binary mixtures, as literature survey reveals that very scarce work has been carried out in concerned with the binary mixtures.

IV.2. EXPERIMENTAL

IV.2.1 Source and purity of samples

[Bu_4PBF_4] of puriss grade was procured from Sigma-Aldrich, Germany and was used as purchased. The mass fraction purity of [Bu_4PBF_4] was ≥ 0.99.

Acetonitrile (ACN) obtained from Merck, India was used after further purification. It was distilled from P_2O_5 and then from CaH_2 in an all-glass distillation apparatus.[IV.22] The middle fraction was collected. About 99% purified acetonitrile with specific conductivity $0.8 - 1.0 \times 10^{-8}$ S cm^{-3} was obtained. The purity of the liquid was checked by measuring it's density and viscosity which were in good agreement with the literature values[IV.22, IV.23] as shown in Table IV.1.

Tetrahydrofuran (THF), Merck, Indian was kept several days over potassium hydroxide (KOH), refluxed for 24 h and distilled over lithium aluminium hydride ($LiAlH_4$) described earlier.[IV.13] The purified solvent had a boiling point of 339 K and a specific conductance of 0.81×10^{-6} S cm^{-3}. The density and viscosity of the purified solvent were in good agreement with the literature data[IV.24, IV.25] as shown in Table IV.1. The purity of the solvent was ≥ 98.9 %.

1,3-dioxolane (1,3-DO) from Merck, containing 0.3 % water and 0.005 % peroxides and sterilized with butylated hydroxytoluene (BHT) was purified by heating under reflux with PbO_2 for 2 h, then cooled and filtered. After adding xylene to the filtrate, the mixture was fractionally distilled.[IV.26] The solvent obtained after purification had a boiling point of 348 K. The density and viscosity of the purified solvent were in good agreement with the literature[IV.27] as shown in Table IV.1. The purity of the solvent finally obtained was ≥ 99.0 %.

IV.2.2 Apparatus and Procedure

All the binary solvent mixtures were prepared by mixing the required volume of ACN, THF and 1,3-DO using the appropriate conversion of the required mass of each solvent into volume at 298.15 K using experimental densities.[IV.28] For the preparation of the solvent mixtures required weighted amount of solvent was transferred to a volumetric flask and the flask was filled up to the mark. The stock solutions of the salt in binary solvent mixtures were prepared by mass (Mettler Toledo AG-285 with uncertainty 0.0003g). For conductance the working solutions, were obtained by mass dilution of the stock solutions. The densities of the solvents and solutions were measured with vibrating-tube density meter (Anton Paar, DMA 4500M), maintained at ±0.01K of the desired temperature and calibrated at the experimental temperature with doubly distilled water and dry air. The uncertainty in density was estimated to be ± 0.00001 g cm^{-3} and the viscosity was measured by means of a suspended Ubbelohde type viscometer, calibrated at 298.15±0.01K with doubly distilled water and purified methanol using density and viscosity value from the literature and the efflux time of flow were recorded with a digital stopwatch correct to ±0.01s. The uncertainty of the viscosity measurements was ±0.003mPas. The details of the methods and experimental techniques had been described elsewhere.[IV.28, IV.30]

The conductance measurements were carried out in a Systronics-308 conductivity bridge of accuracy ±0.01%, using a dip-type immersion conductivity cell, CD-10 having a cell constant of approximately (0.1±0.001) cm^{-1}. Measurements were made in a thermostate water bath maintained at T = (298.15 ± 0.01) K. The cell was calibrated by the method proposed by Lind et al.[IV.31] and cell constant was measured based on 0.01 M aqueous KCl solution.[IV.32] During the conductance measurements, cell constant was maintained within the range 1.10–1.12 cm^{-1}. The conductance data were reported at a frequency of 1 kHz and the accuracy was ±0.3%. During all the measurements, uncertainty of temperatures was ±0.01 K.

The values of relative permittivity (ε_r) of the solvent mixtures were assumed to be an average of those of the pure liquids and calculated using the procedure as described by Rohdewald and Moldner.[IV.33]

IV.3. RESULTS AND DISCUSSION

IV.3.1 Electrical Conductance

IV.3.1.1 Ion-pair formation

The electrolyte was freely soluble in all proportions of the solvent/solvent mixtures. The physical properties of the pure and binary solvent mixtures in different mass fractions at 298.15 K are reported in Table IV.1, where appropriate corrections were made by the specific conductance of the solvents at that temperature.

The specific conductance (κ, μS cm^{-1}) of salt solutions under investigation with a molar concentration within the range of 1.05×10^{-5} - 1.42×10^{-2} M in different mass fractions (w = 0.00, 0.25, 0.50, 0.75, 1.00) were measured. The molar conductance (Λ) for all studied system was calculated using following equation.[IV.34]

$$\Lambda = \frac{1000\ \kappa}{c} \tag{IV.1}$$

where c is the molar concentration and κ is the measured specific conductance of the studied solution. The molar conductances (Λ) of [Bu_4PBF_4] in different binary solvent mixtures were calculated at the corresponding molar concentrations (c) in solvent systems (ACN + THF), (ACN + 1,3-DO) and (THF + 1,3-DO) and given in Table IV.2. For the solvent and solvent mixtures as the range of higher to moderate relative permittivity (ε_r = 35.95 to 14.47), the conductance curves (Λ versus √c) were linear, depicted in Figure IV.1 and extrapolation of √c = 0 evaluated the starting limiting molar conductance for the electrolytes; however, as the relative permittivity (ε_r) dropped to $\varepsilon_r \langle 10$ for pure THF (7.58), 1,3-DO (7.31) and their binary mixture, non-linearity in Figure IV.2, was observed in conductance curves. Thus the conductance data, in (ACN + THF) and (ACN + 1,3-DO) solvent mixtures have been analyzed using the Fuoss conductance equation.[IV.35, IV.36] For a given set of conductivity values $(c_j, \Lambda_j, j = 1,\ldots n)$ three adjustable parameters, the limiting molar conductance (Λ_0), the association constant (K_A) and the distance of closest approach of ions (R) are derived from the following set of equations.

$$\Lambda = P\Lambda_o[(1+R_X)+E_L] \tag{IV.2}$$

$$P = 1-\alpha(1-\gamma) \tag{IV.3}$$

$$\gamma = 1-K_A c\gamma^2 f^2 \tag{IV.4}$$

$$-\ln f = \frac{\beta\kappa}{2(1+\kappa R)} \tag{IV.5}$$

$$\beta = \frac{e^2}{(\varepsilon_r k_B T)} \tag{IV.6}$$

$$K_A = \frac{K_R}{(1-\alpha)} = \frac{K_R}{(1+K_S)} \tag{IV.7}$$

where R_X is the relaxation field effect, E_L is the electrophoretic counter current, k^{-1} is the radius of the ion atmosphere, ε_r is the relative permittivity of the solvent mixture, e is the electron charge, c is the molarity of the solution, k_B is the Boltzmann constant, K_A is the overall paring constant, K_S is the association constant of the contact-pairs, K_R is the association constant of the solvent-separated pairs, γ is the fraction of solute present as unpaired ion, α is the fraction of contact pairs, f is the activity coefficient, T is the absolute temperature and β is twice the Bjerrum distance. The computations were performed using a program suggested by Fuoss. The initial Λ_o values for the iteration procedure were obtained from Shedlovsky extrapolation of the data. Input for the program is the set $(c_j, \Lambda_j, j=1,\dots n), n, \varepsilon, \eta, T$, initial values of Λ_o, and an instruction to cover a pre-selected range of R values.

The best value of a parameter is the one when equations is best fitted to the experimental data corresponding to minimum standard deviation δ for a sequence of predetermined R values, and standard deviation δ was calculated by the following equation

$$\delta^2 = \sum \frac{[\Lambda_j(cal) - \Lambda_j(obs)]^2}{(n-m)} \tag{IV.8}$$

where n is the number of experimental points and m is the number of fitting parameters. The conductance data were analyzed by fixing the distance of closest approach R with two parameter fit ($m = 2$). As for the electrolytes studied in various mass fractions (w_1 = 0.25, 0.50, 0.75, 1.00) of ACN, no significant minima were observed in the δ versus R curves, whereas the R values were arbitrarily preset at the centre to centre distance of solvent-separated ion pair.[IV.21] Thus, R values are assumed to be

$$R = a + d \tag{IV.9}$$

where $a = (r_+ + r_-)$ is the sum of the crystallographic radii of the cation (r_+) and anion (r_-) and d is the average distance corresponding to the side of a cell occupied by a solvent molecule. The distance, d is given by[IV.37]

$$d(\mathring{A}) = 1.183\left(\frac{M}{\rho}\right)^{1/3} \tag{IV.10}$$

where M is the molar mass of the solvent and ρ is its density. For mixed solvents, M is replaced by the mole fraction average molar mass (M_{av}) which is given by

$$M_{av} = \frac{M_1 M_2}{(w_1 M_2 + w_2 M_1)} \tag{IV.11}$$

where w_1 & w_2 is the mass fraction of the first and second component of molar mass M_1 and M_2 respectively. The values of Λ_o, K_A and R obtained by this procedure are represented in Table IV.3. Perusal of Table IV.3 reveals that the limiting molar conductances (Λ_o) of the electrolytes increases with the increase of content of ACN in the solvent mixture with THF and 1,3-DO. The Table also reveals that the association of the [Bu_4PBF_4] is more in 1,3-DO, than THF and ACN, which is in order 1,3-DO > THF > ACN, and its value decreases with increasing content of ACN in their binary mixtures. Hence the ion-solvent interaction increases with the increase in the amount of 1,3-DO and THF in their binary mixtures with ACN, leading to a lower conductance of [Bu_4PBF_4]. The lower viscosity of ACN also supports the above fact because with lower viscosity, the Λ_0 value should increase. The fact is also in line with the increases of the relative permittivity (ε_r) of the solvents/solvent mixtures. Although the decreasing trend of viscosity for the solvent mixtures with increasing content of ACN suggests concomitant increase in limiting molar conductances[IV.37, IV.39] for the electrolyte. The trend suggests solvent viscosity (η_o) is predominance, over the relative permittivity (ε_r), in effecting the electrolytic conductance of the electrolyte under the studied media.

The trend in Λ_0 values can be discussed through another characteristic function called the Walden product ($\Lambda_o\eta$), given in Table IV.3. The decreasing trend of

Walden products with the decreasing amount of ACN in solvent mixture given in Table IV.3 and Figure IV.4 are in accordance with the concomitant increase of viscosity and decreasing limiting molar conductance of the electrolyte in the solvent/solvent mixtures. This is justified as the Walden product of an ion or solute is inversely proportional to the effective solvated radius (r_{eff}) of the ion or solute in a particular solvent/solvent mixture.[IV.40]

$$\Lambda_0\eta = \frac{1}{6\Pi r_{eff} T} \qquad \text{(IV.12)}$$

This points out to the fact that the electrostatic ion-solvent interaction is strong in these cases. The variation of the Walden product reflects the change of solvation.[IV.12,IV.41] Though the variation of the Walden product with solvent composition is difficult to interpret quantitatively, its variation with solvent composition can still be explained by preferential salvation[IV.7, IV.42] of the electrolyte by ACN, THF and 1,3-DO molecules. At low concentration of ACN, the electrolyte are preferentially solvated in THF, 1,3-DO rather than by ACN.

The starting point for most evaluations of ionic conductance is Stokes' law which states that the limiting ionic Walden product ($\lambda_o^{\pm}\eta$), (the limiting ionic conductance-solvent viscosity product) for any singly charged, spherical ion is a function only of the ionic radius and thus, under normal conditions, is a constant. The limiting ionic conductances $\lambda_o^{\pm}$ (for the Bu_4P^+ cation and BF_4^- anion) in different solvent mixtures, mass fraction (w_1 = 0.25, 0.50, 0.75, 1.00) of ACN with THF and 1,3-DO, were calculated using tetrabutylammonium tetraphenylborate (Bu_4NBPh_4) as a 'reference electrolyte' following the scheme as suggested by B. Das et al.[IV.43] We have calculated the limiting ionic conductances $\lambda_o^{\pm}$, in our solvent compositions by interpolation of conductance data from the literature[IV.44] using cubic spline fitting. The $\lambda_o^{\pm}$ values were in turn utilized for the calculation of Stokes' radii (r_S) according to the classical expression[IV.45]

$$r_S = \frac{F^2}{6\pi N_A \lambda_o^{\pm} r_c} \qquad \text{(IV.13)}$$

Ionic Walden products $\lambda_o^{\pm}\eta$, Stokes' radii r_s, and crystallographic radii r_c are presented in Table IV.4. The trends in Walden products $\Lambda_o\eta$ and ionic Walden products $\lambda_o^{\pm}\eta$ for the electrolytes in the solvents/solvent mixtures of ACN with THF and 1,3-DO are depicted in Table IV.3 & IV.4 and Figure IV.4 & IV.5 respectively. It shows that both the ionic Walden products $\lambda_0^{\pm}\eta$ and Walden products $\Lambda_0\eta$ for the electrolyte increase almost linearly as the ACN content increases in the solvent mixtures. For Bu_4P^+ and BF_4^- ion, the Stokes' radii r_s are either lower or comparable to their crystallographic radii r_c, this suggests that the ion are comparatively less solvated than alkali metal ions due to its intrinsic low surface charge density. The distance parameter R, shown in Table IV.3, is the least distance that two free ions can approach before they merge into ion pair. R values have been found to increase with increase in mass fraction of ACN (w_1) in the solvent mixture.

The nature of the curve for the Gibbs energy changes for ion-pair formation, ΔG^o, clearly predicts the tendency for ion-pair formation. The Gibbs energy change ΔG^o is given by the following relationship[IV.46] and is given in Table IV.3.

$$\Delta G^o = - R_g T \ln K_A \qquad \text{(IV.14)}$$

The negative values of ΔG^o can be explained by considering the participation of specific covalent interaction in the ion-association process. The increase in the value of ΔG^o of [Bu_4PBF_4] with increasing amount of ACN in the solvent mixtures leads to the decrease in the ion-solvent interaction.

There are marked characteristic behaviours in the K_A values, which generally decrease as the quantity of ACN is increased in mixtures; the thermal motion probably destroys the solvent structure. However, ion-association for the electrolyte increases as the concentration of THF and 1,3-DO increases in the mixtures.

The schematic representation of ion-solvation, for the particular ion in the studied solvent mixtures (ACN+THF, ACN+1,3-DO), in view of various derived parameters is depicted in **Scheme IV.1,** where w_1 is mass fraction of ACN.

IV.3.1.2 Triple-ion formation

Figure IV.2 presents the graphical representation of Λ vs $\sqrt{c}$; which shows that, the salt follows the same trend, i.e. decreases with increasing concentration, reaches a minimum and then increases. Due to the deviation of the conductometric curves from linearity in case of Bu_4PBF_4 in THF (ε_r = 7.58), 1,3-DO (ε_r = 7.31) and their binary mixtures, the conductance data have been analyzed by the classical Fuoss-Kraus theory of triple-ion formation in the form[IV.37, IV.46]

$$\Lambda g(c)\sqrt{c} = \frac{\Lambda_0}{\sqrt{K_p}} + \frac{\Lambda_0^T K_T}{\sqrt{K_p}}\left(1-\frac{\Lambda}{\Lambda_0}\right)c \qquad \text{(IV.15)}$$

where *g(c)* is a factor that lumps together all the intrinsic interaction terms and is defined by:

$$g(c) = \frac{\exp\{-2.303\,\beta'(c\Lambda)^{0.5}/\Lambda_0^{0.5}\}}{\{1-S(c\Lambda)^{0.5}/\Lambda_0^{1.5}\}(1-\Lambda/\Lambda_0)^{0.5}} \qquad \text{(IV.16)}$$

$$\beta' = \frac{1.8247\times10^6}{(\varepsilon T)^{1.5}} \qquad \text{(IV.17)}$$

$$S = \alpha\,\Lambda_0 + \beta = \frac{0.8204\times10^6}{(\varepsilon T)^{1.5}}\Lambda_0 + \frac{82.501}{\eta(\varepsilon T)^{0.5}} \qquad \text{(IV.18)}$$

In the above equations, Λ_0 is the sum of the molar conductance of the simple ions at infinite dilution, Λ_0^T is the sum of the conductance value of the two triple-ions $[(Bu_4P)_2]^+BF_4$ and $Bu_4P[(BF_4)_2]^-$ for $[Bu_4PBF_4]$ salt; $K_P \approx K_A$ and K_T are the ion-pair and triple-ion formation constants respectively and S is the limiting Onsager coefficient. To make equation IV.15 applicable, the symmetrical approximation of the two possible formation constants of triple-ions, $K_{T1} = \frac{\left[(Bu_4P)_2\right]^+ BF_4}{\left\{\left[Bu_4P^+\right]\left[Bu_4PBF_4\right]\right\}}$ and $K_{T2} = \frac{Bu_4P\left[(BF_4)_2\right]^-}{\left\{\left[BF_4^-\right]\left[Bu_4PBF_4\right]\right\}}$ equal to each other has been adopted, i.e. $K_{T1} = K_{T2} = K_T$[IV.47] and Λ_0 values for the studied electrolyte have been calculated following the scheme as suggested by Krumgalz [1983].[IV.48] The calculated values are listed in Table IV.5. Λ_0^T has been calculated by setting the triple-ion conductance equal to $\frac{2}{3}\Lambda_0$.[IV.49]

The ratio $\frac{\Lambda_0^T}{\Lambda_0}$ was thus set equal to 0.667 during linear regression analysis of equation IV.15. Table IV.5 shows the calculated limiting molar conductance of simple ion (Λ_0), limiting molar conductance of triple ion (Λ_0^T), slope and intercept of equation IV.15 for $[Bu_4PBF_4]$ in THF, 1,3-DO and their binary mixture at 298.15 K. The linear regression analysis of equation IV.15 for the electrolytes with an average regression constant, $R^2 = 0.9653$, gives intercepts and slopes. These values permit the calculation of other derived parameters such as K_P and K_T listed in Table IV.6. A perusal of Table IV.5 shows that the major portion of the electrolytes exists as ion-pairs with a minor portion as triple ions. The tendency of triple ion formation can be judged from the $\left(\frac{K_T}{K_P}\right)$ ratios and $\log\left(\frac{K_T}{K_P}\right)$, which are highest in 1,3-DO. These ratios suggest that strong association between the ions is due to the coulombic interactions as well as to covalent forces in the solution. These results are in good agreement with those of Hazra et al.[IV.50] At very low permittivity of the solvent, i.e., $\varepsilon_r < 10$, electrostatic ionic interactions are very large. So the ion-pairs attract the free cations or anions present in the solution medium as the distance of the closest approach of the ions becomes minimum. These results in the formation of triple-ions, which acquires the charge of the respective ions, attracted from the solution bulk[IV.44, IV.46] i.e.;

$$M^+ + A^- \leftrightarrow M^+ \cdots\cdots\cdots A^- \leftrightarrow MA \qquad (ion\text{-}pair) \qquad \text{(IV.19)}$$
$$MA + M^+ \leftrightarrow MAM^+ \qquad (triple\text{-}ion) \qquad \text{(IV.20)}$$
$$MA + A^- \leftrightarrow MAA^- \qquad (triple\text{-}ion) \qquad \text{(IV.21)}$$

where M^+ and A^- are Bu_4P^+ and BF_4^- respectively. The effect of ternary association[IV.41] thus removes some non-conducting species, MA, from solution, and replaces them with triple-ions which increase the conductance manifested by non-linearity observed in conductance curves for the electrolyte in THF, 1,3-DO and their binary mixtures. The **Scheme IV.2,** depicts the pictorial representation of triple-ion formations for the electrolyte, as an example in THF+1,3-DO binaries.

Furthermore, the ion-pair and triple-ion concentrations, C_P and C_T, respectively of the $[Bu_4PBF_4]$ in THF, 1,3-DO and their binary mixture have also been calculated using the following equations[IV.51]

$$\alpha = \frac{1}{\left(K_P^{1/2} \cdot C^{1/2}\right)} \tag{IV.22}$$

$$\alpha_T = \left(\frac{K_T}{K_P^{1/2}}\right) C^{1/2} \tag{IV.23}$$

$$C_P = C\left(1 - \alpha - 3\alpha_T\right) \tag{IV.24}$$

$$C_T = \left(\frac{K_T}{K_P^{1/2}}\right) C^{3/2} \tag{IV.25}$$

Here, α and α_T are the fraction of ion-pairs and triple-ions present in the salt-solutions are given in Table IV.7. Thus, the values of C_P and C_T given in Table IV.7, indicates that the ions are mainly present as ion-pairs even at high concentration and a small fraction existing as triple-ions. It is also observed that the fraction of the triple-ions in the solution increases with the increasing concentration, in the studied mixed solvent media.

IV.4. CONCLUSIONS

The present work reveals an extensive study on the ion-solvation behaviour of the tetrabutylphosphonium tetrafluoroborate [Bu_4PBF_4] in ACN + THF, ACN + 1,3-DO, and THF + 1,3-DO mixtures through the conductometric measurements. It becomes clear that the electrolyte exists as ion-pairs for former two cases and as triple-ions for latter one. The tendency of the ion-pair and triple-ion formation depends on the size and the charge distribution of the ions. The effective size of the electrolyte increases in THF, 1,3-DO and their binary mixtures due to preferential solvation in such a way that the sizes of the solvated ions follow their crystallographic radii. The degree of ion–solvent interaction also indicates that the salt prefers cyclic ether THF and 1,3-DO than ACN in their solvation or coordination sphere.

REFERENCES

[IV.1] Welton T. Room-temperature ionic liquids. Solvents for synthesis and catalysis. *Chem. Rev.* **1999,** *99,* 2071-2084.

[IV.2] Earle MJ, Seddon KR. Ionic liquids. Green solvents for the future. *Pure Appl. Chem.* **2000,** *72,* 1391-1398.

[IV.3] Dupont J, de Souza RF, Suarez PAZ. Ionic liquid (molten salt) phase organometallic, catalysis. *Chem. Rev.* **2002,** *102,* 3667-3692.

[IV.4] Plechkova NV, Seddon KR, Plechkova NV, Seddon KR. Applications of ionic liquids in the chemical industry. *Chem. Soc. Rev.* **2008,** *37,* 123–150.

[IV.5] Endres F, El Abedin SZ. Air and water stable ionic liquids in physical chemistry. *Phys. Chem. Chem. Phys.* **2006,** *8,* 2101-2116.

[IV.6] Wang P, Zakeeruddin SM, Moser JE, Grätzel M. A new ionic liquid electrolyte enhances the conversion efficiency of dye-sensitized solar cells. *J. Phys. Chem. B,* **2003,** *107,* 13280-13285.

[IV.7] Janz CG, Tomkins RPT. *Non-aqueous Electrolytes Handbook,* Academic Press: New York, **1973,** Vol. 2.

[IV.8] Aurbach, D. *Non-aqueous Electrochemistry,* Marcel Dekker, Inc: New York, **1999.**

[IV.9] Krom, J. A.; Petty, J. T.; Streitwieser, A. Lithium and Cesium Ion-Pair Acidities of Diphenylamine in Tetrahydrofuran. The Aggregation of Lithium and Cesium Diphenylamide. A New Method for the Determination of Aggregation Constants in Dilute Solution. *J. Am. Chem. Soc.* **1993,** *115,* 8024–8030.

[IV.10] Das D, Das B, Hazra DK. Conductance of some 1:1 electrolytes in N,N-dimethylacetamide at 25°C. *J. Solution Chem.* **2002,** *31,* 425- 431.

[IV.11] Guha C, Chakraborty JM, Karanjai S, Das B. The structure and thermodynamics of ion association and solvation of some thiocyanates and nitrates in 2- methoxyethanol studied by conductometry and FTIR spectroscopy. *J. Phys. Chem. B,* **2003,** *107,* 12814–12819.

[IV.12] Das D, Das B, Hazra DK. Electrical conductance of some symmetrical tetraalkylammonium and alkali salts in N, N-dimethylacetamide at 25°C. *J. Solution Chem.* **2003,** *32,* 77–83.

[IV.13] Roy MN, Nandi D, Hazra DK. Conductance studies of alkali metal chlorides and bromides in aqueous binary mixtures of tetrahydrofuran at 25°C. *J. Indian Chem. Soc.* **1993,** *70,* 123–126.

[IV.14] Popvych O, Tomkins RPT. *Nonaqueous Solution Chemistry,* Wiley-Interscience: New York, **1981,** Chapter 4.

[IV.15] Matheson AJ. *Molecular Acoustics,* Wiley-Interscience: London, **1971.**

[IV.16] Das B, Saha N. Electrical conductances of some symmetrical tetraalkylammonium salts in methanol, acetonitrile, and methanol (1)+acetonitrile (2) mixtures at 298.15 K. *J. Chem. Eng. Data.* **2000,** *44,* 2–5.

[IV.17] Roy MN, Pradhan P, Das RK, Guha PG, Sinha B. Ion-pair and triple-ion formation by some tetraalkylammonium iodides in binary mixtures of 1,4-dioxane+tetrahydrofuran. *J. Chem. Eng. Data.* **2008,** *53,* 1417–1420.

[IV.18] Chanda R, Roy MN. Study of ion-solvent interactions of some tetraalkylammonium halides in THF+CCl_4 mixtures by conductance measurements. *Fluid Phase Equilib.* **2008,** *269,* 134–138.

[IV.19] Chen Z, Hojo M. Relationship between triple ion formation constants and the salt concentration of the minimum in the conductometric curves in low-permittivity solvents. *J. Phys. Chem. B* **1997,** *101,* 10896–10902.

[IV.20] Parvatalu D, Srivastava AK. Ionic conductivity in binary solvent mixtures. 6. behavior of selected 1:1 electrolytes in 80 mass propylene carbonate+p-xylene at 25°C. *J. Chem. Eng. Data.* **2003,** *48,* 608–611.

[IV.21] Roy MN, Sinha B, Dakua VK, Sinha A. Electrical conductances of some ammonium and tetraalkylammonium halides in aqueous binary mixtures of 1,4-dioxane at 298.15K. *Pak. J. Sci. Ind. Res.* **2006,** *49,* 153–159.

[IV.22] Saha N, Das B, Apparent molar volumes of some symmetrical tetraalkylammonium bromides in acetonitrile at (298.15, 308.15, and 318.15)K. *J. Chem. Eng. Data.* **1997,** *42,* 227-229.

[IV.23] Prolongo MG, Masegosa RM, Fuentes IH, Horta A. Viscosities and excess volumes of binary mixtures formed by the liquids acetonitrile, pentyl acetate, 1-chlorobutane, and carbon tetrachloride at 25°C. *J. Phys. Chem.* **1984,** *88,* 2163-2167.

[IV.24] Roy MN, Dey R, Jha A. Study of ion-solvent interactions of some alkali metal chlorides in tetrahydrofuran+water mixture at different temperatures. *J. Chem. Eng. Data.* **2001,** *46,* 1327-1329.

[IV.25] Sinha, A.; Roy, M. N.; Studies of Viscous Antagonism, Excess Molar Volume and Isentropic Compressibility in Aqueous Mixed Solvent Systems at Different Temperatures. *Phys. Chem. Liq.* **2006,** *44,* 303-314.

[IV.26] Roy MN, Sinha A. Viscous synergy and antagonism and isentropic compressibility of ternary mixtures containing 1,3-dioxolane, water and monoalkanols at 303.15 K. *Fluid Phase Equilib.* **2006,** *243,* 133-141.

[IV.27] Roy MN, Ekka D, Dewan R. Ionic solvation of tetrabutylammonium hexafluorophosphate in pure nitromethane, 1,3-dioxolane and nitrobenzene: A comparative physicochemical study. *Fluid Phase Equilibria.* **2012,** *314,* 113– 120.

[IV.28] Roy MN, Dewan R, Sarkar L. Ion-solvent interactions of some halides of common cations with organic solvent mixtures by conductometric, volumetric, viscometric, and refractometric techniques. *J. Chem. Eng. Data.* **2010,** *55,* 1347–1353.

[IV.29] Sinha B, Sarkar BK, Roy MN. Apparent molar volumes and viscosity *B*-coefficients of nicotinamide in aqueous tetrabutylammonium bromide solutions at *T*= (298.15, 308.15, and 318.15) K. *J. Chem. Thermodyncs.* **2008,** *40,* 394–400.

[IV.30] Bhattacharjee A, Roy MN. Ion Association and Solvation Behavior of Tetraalkylammonium Iodides in Binary Mixtures of Dichloromethane + N, N-Dimethylformamide Probed by a Conductometric Study. *Phys. Chem. Chem. Phys.* **2010,** *12,* 14534–14542.

[IV.31] Lind Jr. JE, Zwolenik JJ, Fuoss RM. Calibration of conductance cells at 25° with aqueous solutions of potassium chloride. *J. Am. Chem. Soc.* **1959,** *81,* 1557-1559.

[IV.32] Roy MN, Banerjee A, Das RK. Conductometric study of some alkali metal halides in dimethyl sulfoxide + acetonitrile at T = 298.15 K. *J. Chem. Thermodyncs.,* **2009,** *41,* 1187-1192.

[IV.33] Rohdewald P, Moldner M. Dielectric Constants of Amide-Water Systems. *J. Phys. Chem.* **1973,** *77,* 373–377.

[IV.34] El-Dossoki FI, Effect of hydrogen bond, relative permittivity and temperature on the transport properties and the association behavior of some 1:1 electrolytes in some binary mixed solvents. *J. Mol. Liquids.* **2010,** *151,* 1–8.

[IV.35] Fuoss RM. Paired ions: Dipolar pairs as subset of diffusion pairs. *Proc. Natl. Acad. Sci. U.S.A.* **1978,** *75,* 16–20.

[IV.36] Fuoss RM. Conductance-concentration function for the paired ion model. *J. Phys. Chem.* **1978,** *82,* 2427–2440.

[IV.37] Fuoss RM, Accascina F. *Electrolytic Conductance,* Interscience: New York, **1959.**

[IV.38] Covington AK, Dickinson T. *Physical chemistry of organic solvent systems,* Plenum: New York, **1973.**

[IV.39] Bockris JO, Reddy AN. *Modern Electrochemistry,* 2nd Ed. Plenum Press: New York, **1998,** p 552.

[IV.40] Bhat JI, Bindu P. Effect of temperature on the conductance of Chloramine-T and Bromamine-T in different compositions of solvent mixtures. *J. Ind. Chem. Soc.* **1995,** *72,* 783-790.

[IV.41] Sinha A, Roy MN. Conductivity studies of sodium iodide in pure tetrahydrofuran and aqueous binary mixtures of tetrahydrofuran and 1,4-dioxane at 298.15 K. *Phys. Chem. Liq.* **2007,** *45,* 67-77.

[IV.42] Inoue N, Xu M, Petrucci S. Temperature dependence of ionic association and of molecular relaxation dynamics of lithium hexafluoroarsenate in 2-methyltetrahydrofuran. *J. Phys. Chem.* **1987,** *91,* 4628-4635.

[IV.43] Chakraborty JM, Das B. Electrical conductances and viscosities of tetrabutylammonium thiocyanate in acetonitrile in the temperature range 25–45°C. *Z. Phys. Chem.* **2004,** *218,* 219–230.

[IV.44] Fuoss RM, Hirsch E. Single Ion Conductances in Non-aqueous Solvents. *J. Am. Chem. Soc.* **1960,** *82,* 1013–1017.

[IV.45] Robinson RA, Stokes RH. *Electrolyte Solutions,* Butterworth: London, **1959,** Ch 6, p 130.

[IV.46] Fuoss RM, Kraus CA, Properties of electrolytic solutions. IV. The conductance minimum and the formation of triple ions due to the action of coulomb forces. *J. Am. Chem. Soc.* **1933,** *55,* 2387–2399.

[IV.47] Harada Y, Salamon M, Petrucci S. Molecular dynamlcs and ionic associations of $LiAsF_6$ in 4-butyrdactone mixtures with 2-methyitetrahydrofuran. *J. Phys. Chem.* **1985,** *89,* 2006–2010.

[IV.48] Krumgalz BS. Separation of limiting equivalent conductances into ionic contributions in non-aqueous solutions by indirect methods. *J. Chem. Soc, Faraday Trans. I,* **1983,** *79,* 571–587.

[IV.49] Delsignore M, Farber H. Ionic conductivity and microwave dielectric relaxation of LiAsF6and LiClO4in dimethyl carbonate. *J. Phys. Chem.,* **1985,** *89,* 4968–4973.

[IV.50] Nandi D, Roy MN, Hazra DK. Electrical conductances for tetraalkylammonium bromides, $LiBF_4$ and $LiAsF_6$ in tetrahydrofuran at 25°C. *J. Indian Chem. Soc.* **1993,** *70,* 305-310.

[IV.51] Nandi D, Das S, Hazra DK. *Ind. J. Chem. A.* **1988,** *27,* 574–580.

[IV.52] Philip PR, Jolicoeur C. Near-infrared study of the state of water in aqueous solutions of tetraalkylammonium and -phosphonium bromides and alkali halides at 10, 25, and 40.deg. *J. Phy. Chem.* **1973,** *77(26),* 3071-3077.

[IV.53] Libus W, Chachulski B, Fraczyk L. Electrical conductance and ionic association of the bivalent transition metal tetrafluoroborates in acetonitrile solution. *J. Sol. Chem.* **1980,** *9(5),* 355-369.

TABLES

Table IV.1: Values of Density (ρ), Viscosity (η) and Relative Permittivity (ε_r) of ACN, THF, 1,3-DO and their binary mixtures where w_1, w_2 and w_3 are the mass fraction of ACN, THF and 1,3-DO respectively at T = 298.15 K

Solvents	$\rho \times 10^{-3}$ /kg·m^{-3})		η /mPa·s		ε_r
	Expt	Lit	Expt	Lit	
w_1 = 1.00	0.77668	0.77667[IV.22]	0.344	0.3446[IV.22]	35.95[IV.38]
w_2 = 1.00	0.88074	0.88072[IV.24]	0.463	0.4630[IV.25]	7.58[IV.38]
w_3 = 1.00	1.05873	1.05873[IV.27]	0.589	0.5892[IV.27]	7.31[IV.38]
ACN(1) + THF(2)					
w_1 = 0.25	0.85473		0.433		14.67^a
w_1 = 0.50	0.82871		0.404		21.77^a
w_1 = 0.75	0.80269		0.374		28.86^a
ACN(1) + 1,3-DO(3)					
w_1 = 0.25	0.98822		0.528		14.47^a
w_1 = 0.50	0.91770		0.467		21.63^a
w_1 = 0.75	0.84719		0.406		28.79^a
THF(2) + 1,3-DO(3)					
w_2 = 0.25	1.01423		0.558		7.38^a
w_2 = 0.50	0.96974		0.526		7.45^a
w_2 = 0.75	0.92524		0.495		7.51^a

^{a} Obtained by interpolation of literature data from Ref. [IV.33].

Table IV.2: Molar conductance (Λ) and the corresponding concentration (c) of Bu$_4$PBF$_4$ in ACN, THF, 1,3-DO and their binary mixtures where w_1, w_2 and w_3 are the mass fraction of ACN, THF and 1,3-DO respectively at T = 298.15 K

$c\times10^4$ /mol·dm^{-3}	$\Lambda\times10^4$ S·m^2·mol^{-1}	$c\times10^4$ /mol·dm^{-3}	$\Lambda\times10^4$ S·m^2·mol^{-1}	$c\times10^4$ /mol·dm^{-3}	$\Lambda\times10^4$ S·m^2·mol^{-1}
Acetonitrile		Tetrahydrofuran		1,3-Dioxolane	
9.32	167.16	0.25	27.73	0.11	19.95
17.09	165.08	0.38	24.18	0.21	16.50
23.66	163.92	0.55	20.96	0.30	14.08
29.29	162.75	0.70	18.54	0.39	12.25
34.18	162.07	0.90	16.27	0.46	10.75
42.22	160.81	1.01	15.08	0.57	9.42
48.57	160.00	1.16	13.71	0.69	8.62
55.93	158.89	1.34	12.65	0.83	8.23
63.10	158.13	1.48	12.15	0.94	9.52
70.49	157.26	1.66	12.06	1.03	10.99
77.52	156.45	1.91	13.03	1.12	13.41
82.98	155.90	2.16	15.48	1.20	15.65
ACN(1) + THF(2)					
w_1 = 0.25		w_1 = 0.50		w_1 = 0.75	
27.01	81.80	19.57	109.89	13.63	137.12
36.30	79.80	28.81	107.06	22.35	134.91
47.16	77.75	37.21	105.07	29.98	132.90
58.07	75.80	47.75	103.04	39.11	130.92
67.75	74.81	56.65	101.35	46.40	129.87
76.67	73.41	64.12	100.31	54.82	128.41
88.57	72.26	70.46	99.50	60.77	127.81
97.17	71.15	78.78	98.07	68.66	126.46
103.98	70.25	86.34	96.91	76.00	125.35
112.17	69.10	93.74	95.96	81.43	124.46

118.59	68.40	103.53	95.00	88.93	123.75
125.73	68.02	109.94	94.05	94.38	123.14
		ACN(1) + 1,3-DO(3)			
$w_1 = 0.25$		$w_1 = 0.50$		$w_1 = 0.75$	
31.42	77.22	22.56	104.82	15.81	133.75
40.07	75.70	31.58	102.30	21.09	132.20
48.72	74.27	41.34	100.41	28.84	130.19
57.46	72.88	49.70	98.81	37.45	128.38
68.06	71.39	60.53	96.90	45.70	126.99
77.26	70.10	70.73	95.22	54.46	125.29
89.11	68.56	80.46	93.60	62.73	123.98
100.60	66.89	88.55	92.42	70.73	122.70
113.42	65.53	97.81	91.30	77.44	121.79
121.88	64.61	108.58	89.77	85.43	120.76
131.79	63.72	117.87	88.80	91.81	119.82
140.42	62.89	124.19	88.00	99.76	118.84
		THF(2) + 1,3-DO(3)			
$w_2 = 0.25$		$w_2 = 0.50$		$w_2 = 0.75$	
0.13	22.52	0.16	23.87	0.20	25.56
0.22	19.28	0.26	20.86	0.31	22.25
0.32	16.63	0.35	18.65	0.42	19.89
0.45	14.10	0.44	16.63	0.58	16.96
0.58	12.28	0.56	14.72	0.71	15.30
0.73	10.77	0.70	13.09	0.88	13.46
0.87	9.84	0.84	11.77	1.08	11.95
1.01	9.67	1.03	10.67	1.27	11.13
1.14	10.02	1.23	10.82	1.44	10.96
1.23	10.85	1.39	11.74	1.57	11.63
1.38	13.99	1.52	13.73	1.70	13.09
1.48	17.09	1.64	16.84	1.84	15.98

Table IV.3: Limiting molar conductivity (Λ_0), the association constant (K_A), the distance of closest approach of ions (R), Standard Deviations δ of Experimental Λ from Equation (IV.1), Walden Product ($\Lambda_0\eta$) and free energy change (ΔG^o) of Bu_4PBF_4 in ACN and its binary mixtures with THF, 1,3-DO, where w_1 are the mass fraction of ACN at T = 298.15 K

Solvents	$\Lambda_0 \times 10^4$ /S·m²·mol⁻¹	$K_A \times 10^{-4}$ /dm²·mol⁻¹	R /Å	δ	$\Lambda_0\eta \times 10^4$ /S·m²·mol⁻¹·mPa·s	ΔG^0 /kJ·mol⁻¹
w_1 = 1.00	167.99	10.42	12.14	0.36	57.85	-2.86
			ACN(1) +THF(2)			
w_1 = 0.25	87.88	30.65	12.10	0.22	38.09	-3.13
w_1 = 0.50	114.26	24.33	11.91	0.36	46.13	-3.07
w_1 = 0.75	139.56	16.59	11.76	0.38	52.21	-2.98
			ACN(1) + 1,3-DO(3)			
w_1 = 0.25	88.95	34.09	11.89	0.24	44.86	-3.15
w_1 = 0.50	110.44	26.14	11.77	0.17	51.55	-3.09
w_1 = 0.75	136.93	18.04	11.69	0.32	55.54	-3.00

Table IV.4: Limiting Ionic Conductance ($\lambda_o^{\pm}$), Ionic Walden Product ($\lambda_o^{\pm}\eta$), Stokes' Radii (r_s) and Crystallographic Radii (r_c) of Bu₄PBF₄ in ACN and its binary mixtures with THF, 1,3-DO, where w_1 are the mass fraction of ACN at T = 298.15 K

Solvents	Ion	$\lambda_o^{\pm}$ /S·m²·mol⁻¹	$\lambda_o^{\pm}\eta$ /S·m²·mol⁻¹·mPa·s	r_s /Å	$^b r_c$ /Å
w_1 = 1.00	Bu_4P^+	64.86	22.34	3.67	4.42
	BF_4^-	103.12	35.52	2.31	2.78
		ACN(1) + THF(2)			
w_1 = 0.25	Bu_4P^+	33.93	14.71	5.57	4.42
	BF_4^-	53.95	23.38	3.50	2.78
w_1 = 0.50	Bu_4P^+	44.12	17.81	4.60	4.42
	BF_4^-	70.15	28.32	2.89	2.78
w_1 = 0.75	Bu_4P^+	53.89	20.16	4.06	4.42
	BF_4^-	85.67	32.05	2.56	2.78
		ACN(1) + 1,3-DO(3)			
w_1 = 0.25	Bu_4P^+	32.80	17.32	4.73	4.42
	BF_4^-	52.15	27.54	2.98	2.78
w_1= 0.50	Bu_4P^+	42.64	19.91	4.12	4.42
	BF_4^-	67.80	31.65	2.59	2.78
w_1 = 0.75	Bu_4P^+	52.87	21.44	3.82	4.42
	BF_4^-	84.06	34.10	2.40	2.78

[b] Crystallographic radii of cation and anion from Ref. [IV.52] and [IV.53] respectively.

Table IV.5: The calculated limiting molar conductance of ion-pair (Λ_0), limiting molar conductance of triple-ion (Λ_0^T), slope and intercept of Equation (IV.15) of Bu_4PBF_4 in THF, 1,3-DO and their binary mixture, where w_2 and w_3 are mass fraction of THF and 1,3-DO at T = 298.15 K

Solvents	$\Lambda_0 \times 10^4$ /S·m²·mol⁻¹	$\Lambda_0^T \times 10^4$ /S·m²·mol⁻¹	Slope×10⁻²	Intercept
w_2 = 1.00	74.93	49.98	0.82	0.15
w_3 = 1.00	43.85	29.25	6.19	0.07
THF(2) + 1,3-DO(3)				
w_2 = 0.25	46.98	31.34	4.64	0.09
w_2 = 0.50	52.78	35.20	3.81	0.10
w_2 = 0.75	61.36	40.93	1.70	0.12

Table IV.6: Salt concentration at the minimum conductivity (c_{min}) along with the ion-pair formation constant (K_P), triple-ion formation constant (K_T) of Bu_4PBF_4 in THF, 1,3-DO and their binary mixture, where w_2 and w_3 are mass fraction of THF and 1,3-DO at T = 298.15 K

Solvent /solvent mixture	c_{min}×10⁴ /mol·dm⁻³	log c_{min}	K_P ×10⁻⁴ /m³·mol⁻¹	K_T×10⁻³ /m³·mol⁻¹	$\left(\frac{K_T}{K_P}\right)$ ×10³	log $\left(\frac{K_T}{K_P}\right)$
w_2 = 1.00	1.66	-3.78	25.36	0.83	3.27	-2.49
w_3 = 1.00	0.83	-4.08	45.35	14.26	31.43	-1.50
		THF(2) + 1,3-DO(3)				
w_2 = 0.25	1.01	-3.99	28.99	7.98	27.53	-1.56
w_2 = 0.50	1.03	-3.98	25.76	5.49	21.32	-1.67
w_2 = 0.75	1.44	-3.84	23.92	2.03	8.50	-2.07

Table IV.7: Salt concentration (c_{min}) at the minimum conductivity (Λ_{min}), the ion-pair fraction (α), triple-ion fraction (α_T), ion-pair concentration (C_P) and triple-ion concentration (C_T) of Bu_4PBF_4 in THF, 1,3-DO and their binary mixture, where w_2 and w_3 are mass fraction of THF and 1,3-DO at T = 298.15 K

Solvent /solvent mixture	$c_{min}\times10^4$ /mol·dm^{-3})	$\Lambda_{min}\times10^4$	α	α_T	$C_P\times10^5$ /mol·dm^{-3}	$C_T\times10^6$ /mol·dm^{-3}
w_2 = 1.00	1.66	12.06	0.153	0.021	15.14	3.54
w_3 = 1.00	0.83	8.23	0.162	0.193	11.78	16.06
		THF(2) + 1,3-DO(3)				
w_2 = 0.25	1.01	9.67	0.184	0.149	12.77	15.09
w_2 = 0.50	1.03	10.67	0.193	0.110	11.75	11.38
w_2 = 0.75	1.44	10.96	0.170	0.049	14.04	7.15

Figures

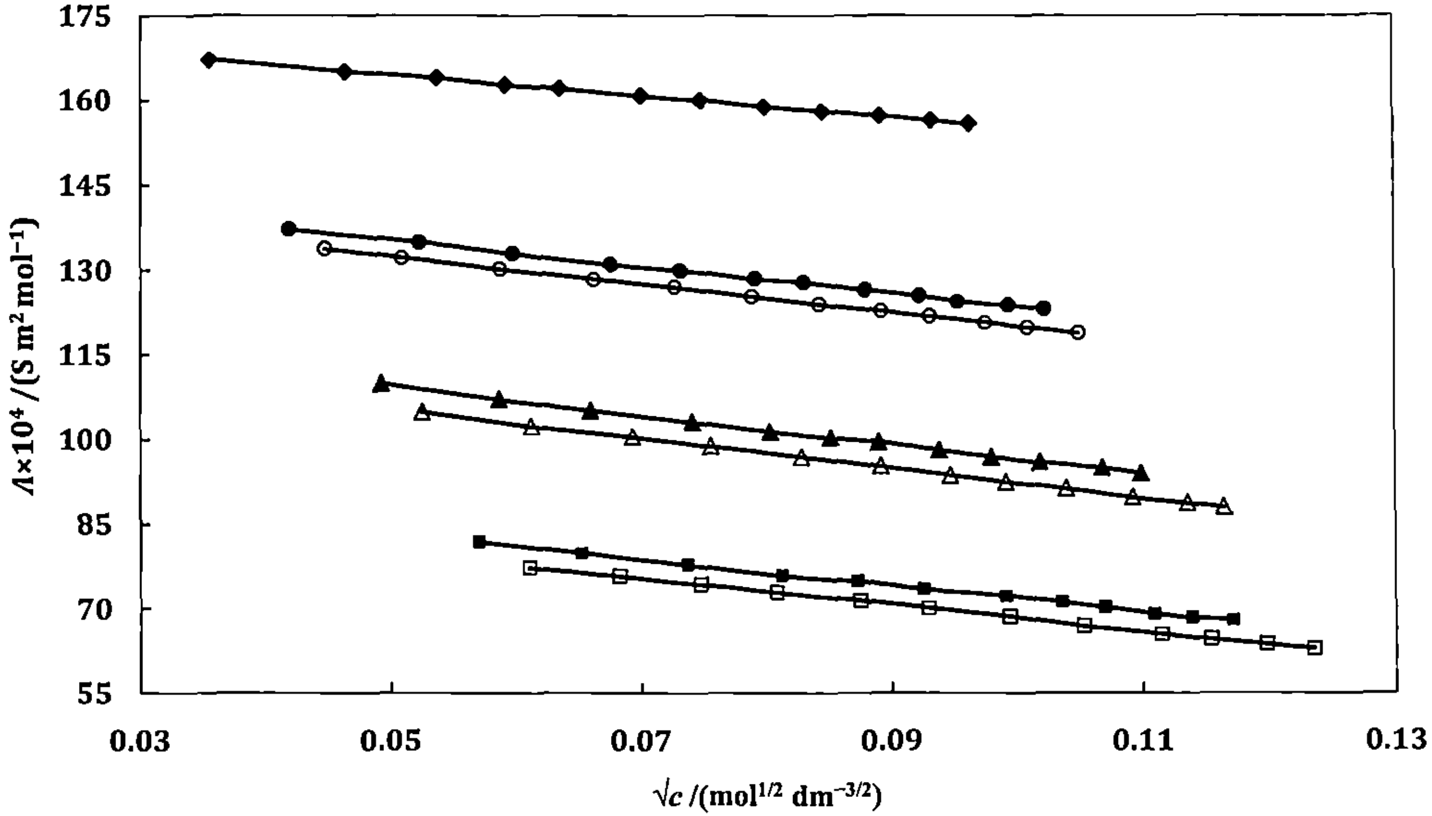

Figure IV.1: Plot of molar conductance (Λ) and the square root of concentration ($\sqrt{c}$) of Bu_4PBF_4 in w_1=0.25 (■), w_1=0.50 (▲), w_1=0.75 (●), w_1=1.00 (♦) of ACN in THF and w_1=0.25 (□), w_1=0.50 (Δ), w_1=0.75 (○), w_1=1.00 (♦) of ACN in 1,3-DO at T = 298.15K

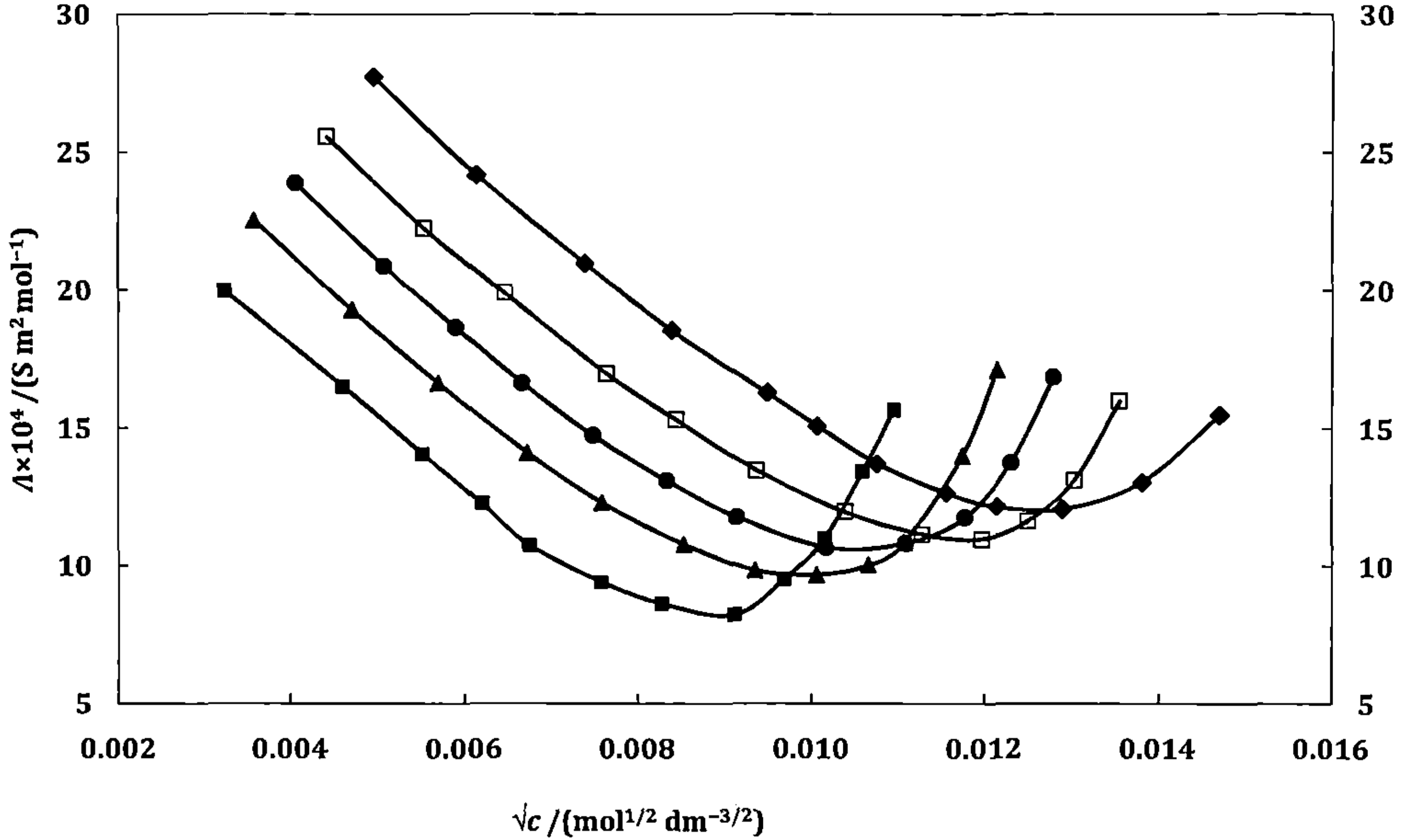

Figure IV.2: Plot of molar conductance (Λ) and the square root of concentration ($\sqrt{c}$), of Bu_4PBF_4 in w_2=0.00 (■), w_2=0.25 (▲), w_2=0.50 (●), w_2=0.75 (□), w_2=1.00 (♦) of THF in 1,3-DO at T = 298.15K

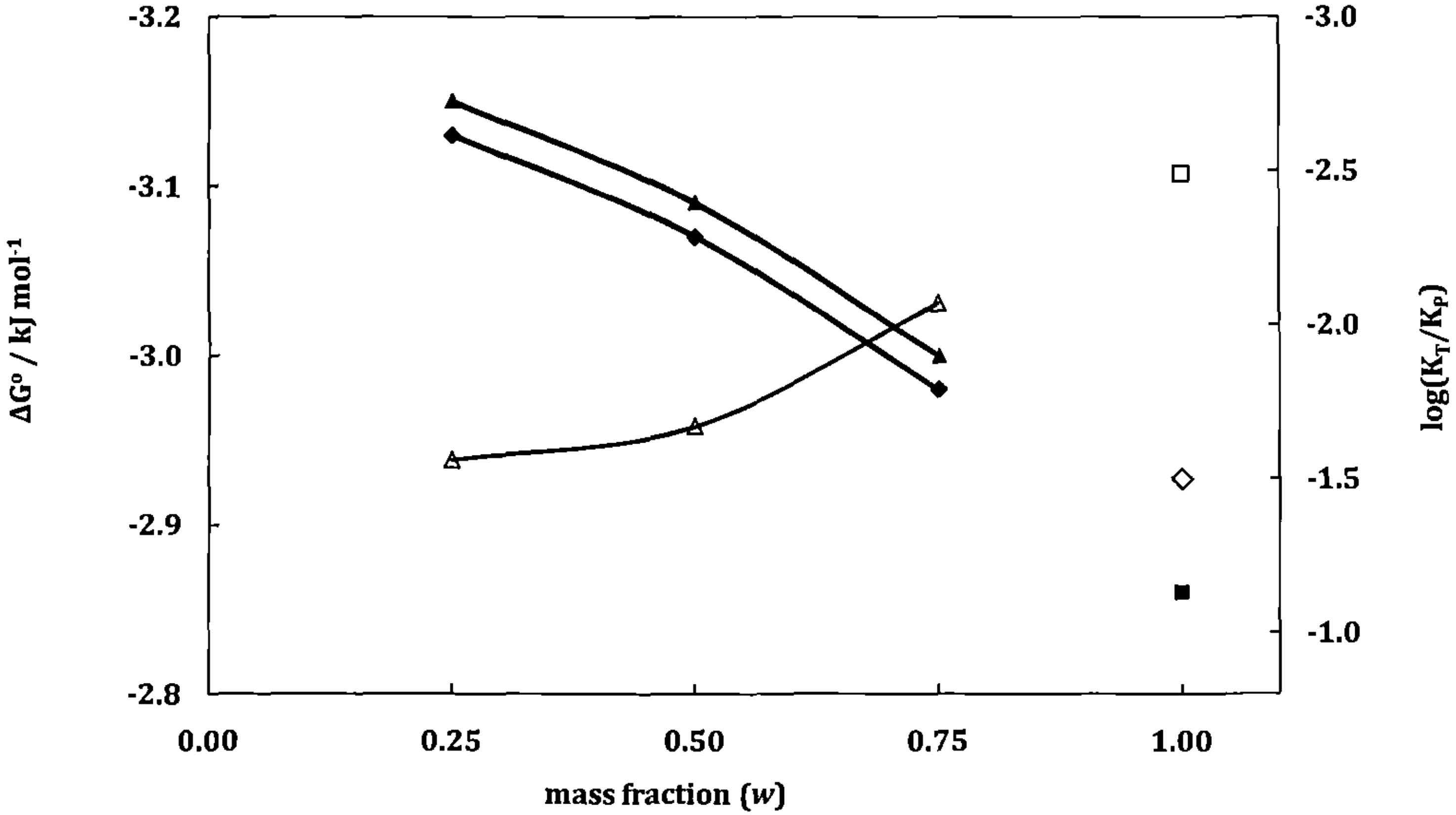

Figure IV.3: Plot of the free energy change (ΔG^o) vs mass fraction (w), of Bu_4PBF_4 in ACN (■), ACN+ THF (♦), ACN+1,3-DO (▲), and $\log(K_T/K_P)$ vs mass fraction of Bu_4PBF_4 in THF (□), in 1,3-DO (◊) and their binary mixture (Δ) at T = 298.15 K

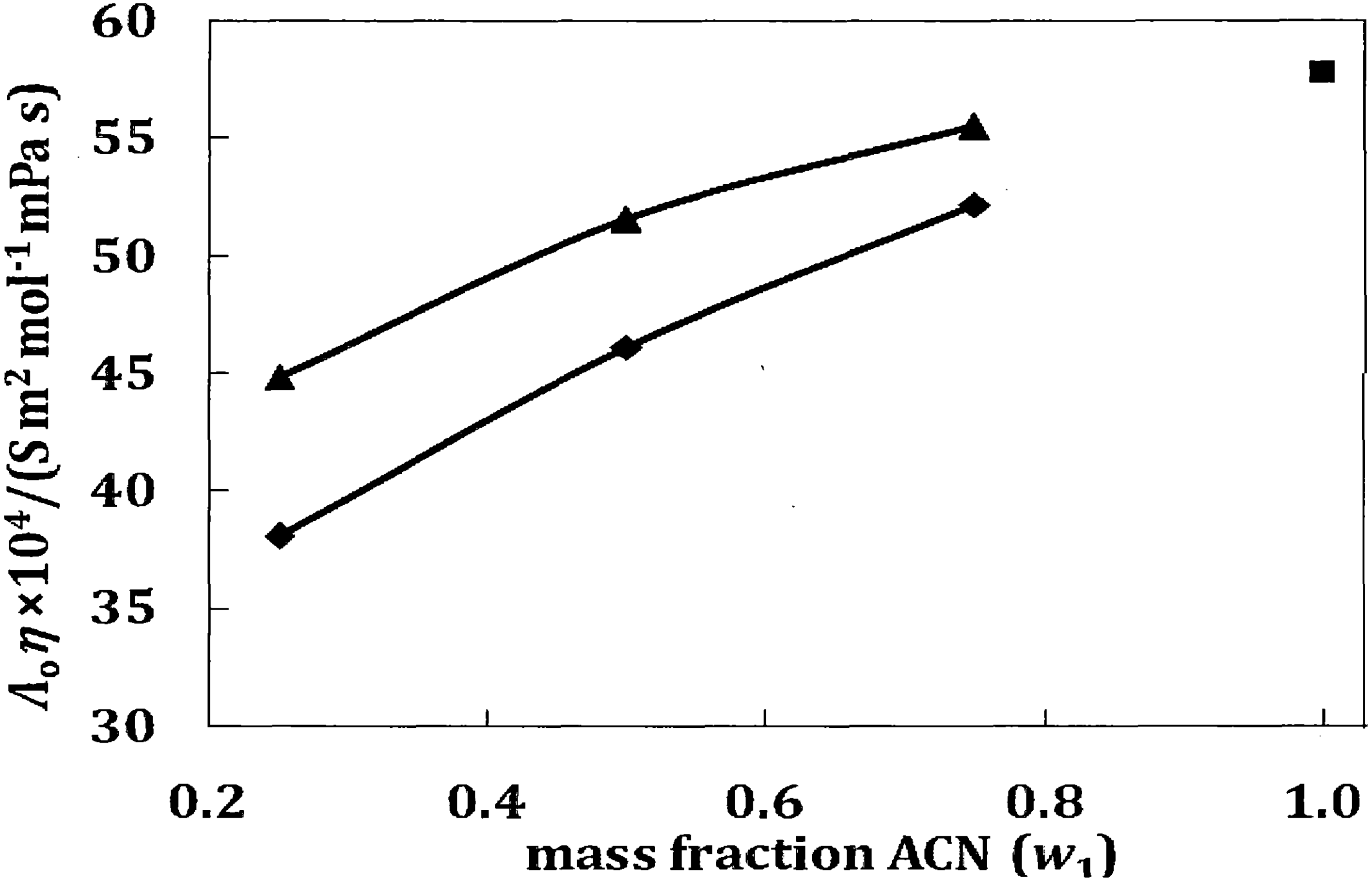

Figure IV.4: Plot of Walden Product ($\Lambda_0\eta$) vs mass fraction of ACN (w_1) for Bu_4PBF_4 in ACN (■), ACN+ THF (♦), ACN+1,3-DO (▲) at T = 298.15 K

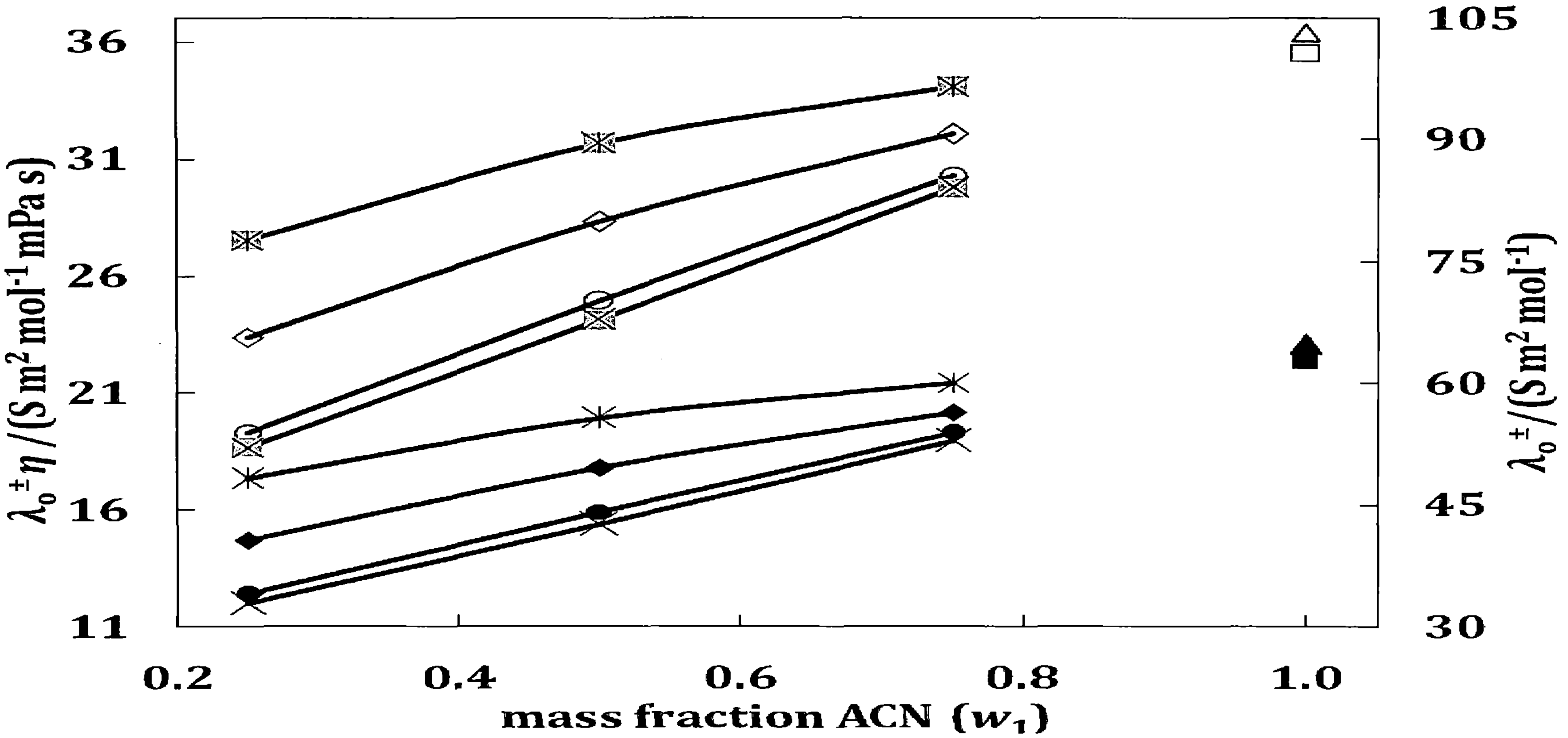

Figure IV.5: Plot of ionic Walden Product ($\lambda_o^{\pm}\eta$) vs mass fraction (w), for Bu_4P^+ in ACN (■), ACN+THF (♦), ACN+1,3-DO (✳) and for BF_4^- in ACN (□), ACN+THF (◊), ACN+1,3-DO (☒); and Plot of limiting ionic conductance ($\lambda_o^{\pm}$) vs mass fraction (w), for Bu_4P^+ in ACN (▲), ACN+THF (●), ACN+1,3-DO (×) and for BF_4^- in ACN (Δ), ACN+THF (○), ACN+1,3-DO (☒); at T = 298.15 K

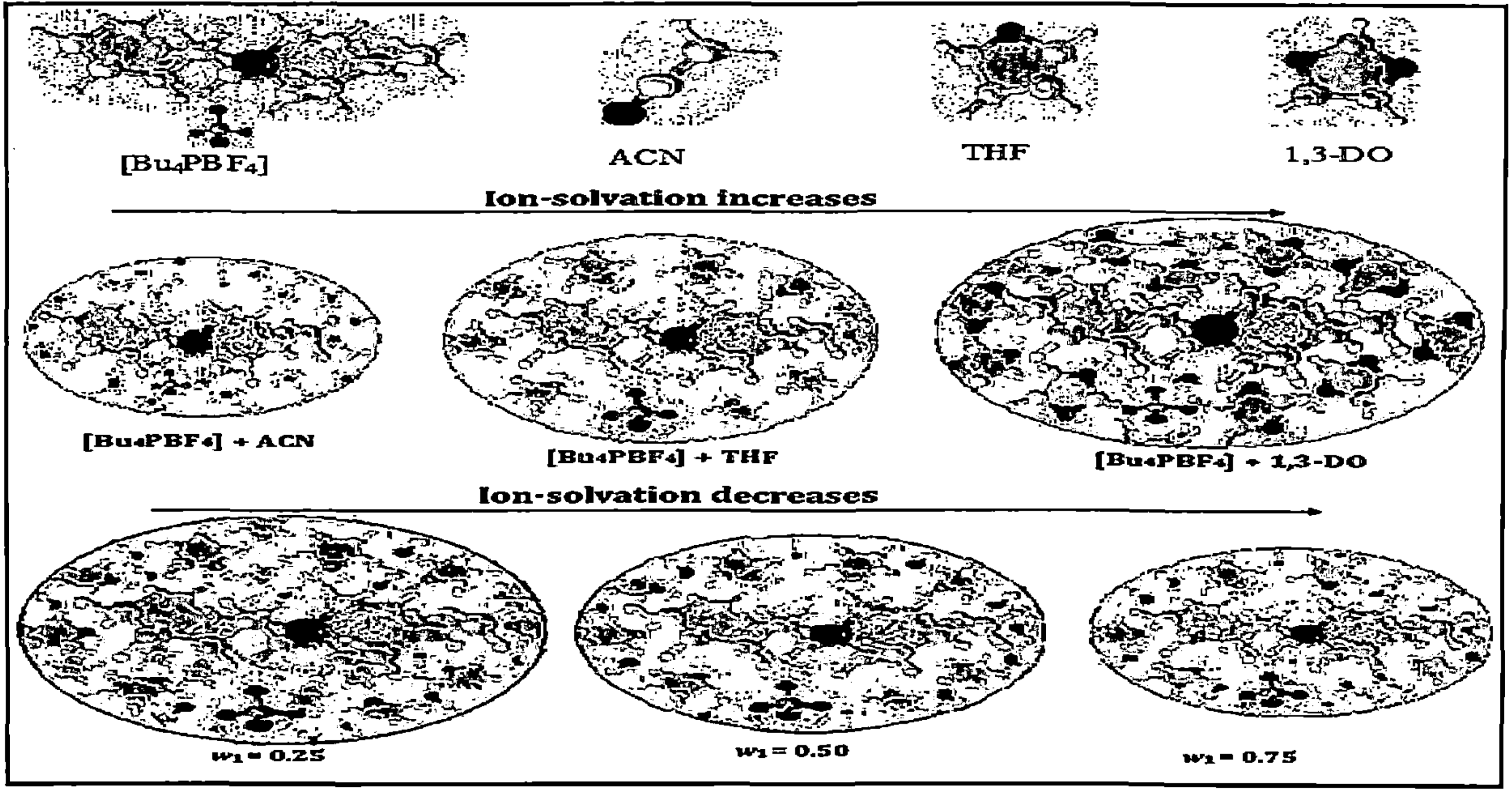

Scheme IV.1: The schematic representation of ion-solvation, for the particular ion in the studied solvent mixtures (ACN+THF, ACN+1,3-DO), in view of various derived parameters is depicted in, where w_1 is mass fraction of ACN

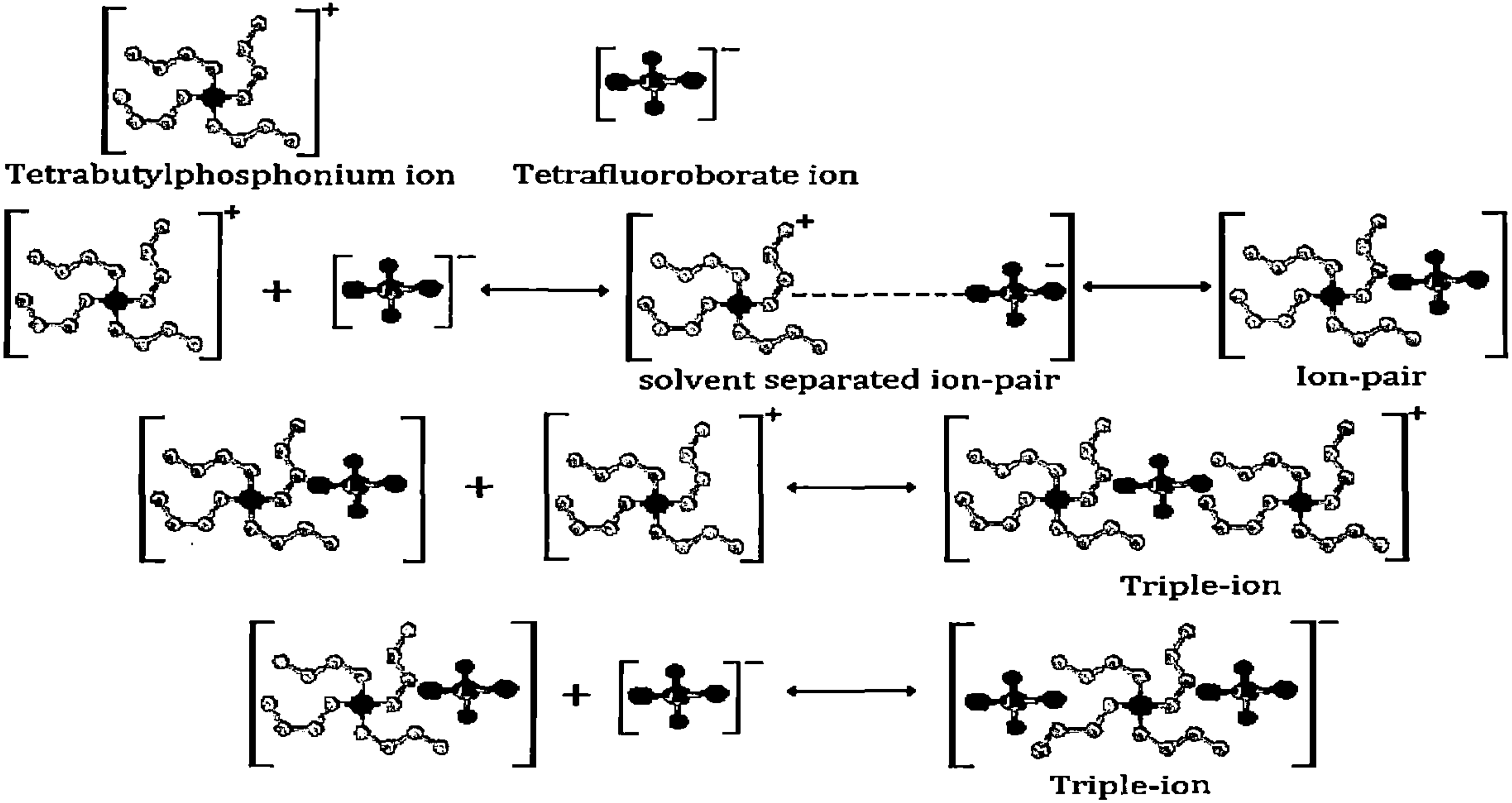

Scheme IV.2: The pictorial representation of triple-ion formations for the electrolyte, as an example in THF+1,3-DO binaries